Original Research *Highlight article*

Telmisartan ameliorates cardiac fibrosis and diastolic function in cardiorenal heart failure with preserved ejection fraction

Di Chang, Ting-Ting Xu, Shi-Jun Zhang, Yu Cai, Shu-Dan Min, Zhen Zhao, Chun-Qiang Lu, Yuan-Cheng Wang and Shenghong Ju

Jiangsu Key Laboratory of Molecular and Functional Imaging, Department of Radiology, Zhongda Hospital, Medical School of Southeast University, Nanjing 210009, China

Corresponding author: Shenghong Ju. Email: jsh0836@hotmail.com

Impact statement

Approximately two-thirds of patients with heart failure have CKD, making CKD a major contributor to the occurrence and development of HFpEF. Unfortunately, the underlying mechanism of cardiorenal HFpEF is still elusive. In this study, we demonstrated that cardiac fibrosis exerts a critical role in the pathology of cardiorenal HFpEF. In addition, RAAS modulation with Telmisartan is capable of ameliorating cardiac remodeling and preserving diastolic dysfunction in the development of cardiorenal HFpEF, possibly or partly via the inhibition of cardiac inflammatory–fibrosis process.

Abstract

Chronic kidney disease (CKD) is a major contributor to the development of heart failure with preserved ejection fraction (HFpEF), whereas the underlying mechanism of cardiorenal HFpEF is still elusive. The aim of this study was to investigate the role of cardiac fibrosis in a rat model of cardiorenal HFpEF and explore whether treatment with Telmisartan, an inhibitor of renin-angiotensin-aldosterone system (RAAS), can ameliorate cardiac fibrosis and preserve diastolic function in cardiorenal HFpEF. Male rats were subjected to 5/6 subtotal nephrectomy (SNX) or sham operation (Sham), and rats were allowed four weeks to recover and form a stable condition of CKD. Telmisartan or vehicle was then administered p. o. (8 mg/kg/d) for 12 weeks. Blood pressure, brain natriuretic peptide (BNP), echocardiography, and cardiac magnetic resonance imaging were acquired to evaluate cardiac structural and functional alterations. Histopathological staining, real-time polymerase chain reaction (PCR) and western blot were performed to evaluate cardiac remodeling. SNX rats showed an HFpEF phenotype with increased BNP, decreased early to late diastolic transmitral flow velocity (E/A) ratio, increased left ventricular (LV) hypertrophy and preserved ejection fraction (EF). Pathology revealed increased cardiac fibrosis in cardiorenal HFpEF rats compared with the Sham group, while chronic treatment with Telmisartan significantly decreased cardiac fibrosis, accompanied by reduced markers of fibrosis (collagen I and collagen III) and profibrotic cytokines (α-smooth muscle actin, transforming growth factor-β1, and connective tissue growth factor). In addition, myocardial inflammation was decreased after Telmisartan treatment, which was in a linear correlation with cardiac fibrosis. Telmisartan also reversed LV hypertrophy and E/A ratio, indicating that Telmisartan can improve LV remodeling and diastolic function in cardiorenal HFpEF. In conclusion, cardiac fibrosis is central to the pathology of cardiorenal HFpEF, and RAAS modulation with Telmisartan is capable of alleviating cardiac fibrosis and preserving diastolic dysfunction in this rat model.

Keywords: Heart failure with preserved ejection fraction, cardiorenal syndrome, diastolic function, chronic kidney disease, cardiac fibrosis, renin-angiotensin-aldosterone system

Experimental Biology and Medicine **2021; 246: 2511–2521. DOI: 10.1177/15353702211035058**

Introduction

Heart failure (HF) with preserved ejection fraction (HFpEF) is increasing in prevalence.[1] As a clinical disorder that accounts for nearly half of all HF cases, HFpEF has recently attracted more and more attention.[2,3] With a much more insidious evolution of HFpEF than that of HF with reduced ejection fraction (HFrEF), it is recognized that HFpEF is a multi-organ disease with a huge unmet need in both the understanding of the pathobiological mechanisms and the selection of the treatment strategies.[4–6] The fundamental pathogenesis of HFpEF is heterogeneous, which is associated with different phenotypes including aging and diverse

concomitant comorbidities such as hypertension, diabetes and chronic kidney disease (CKD).[7–9] In clinical practice, approximately two-thirds of HF patients have CKD, making CKD a major contributor to the occurrence and development of HFpEF,[10] which is called cardiorenal HFpEF. However, the underlying mechanism of cardiorenal HFpEF is still elusive and remains to be elucidated.

Cardiac fibrosis is central to the pathology of HF, and fibrosis is characterized by extracellular matrix (ECM) expansion and remodeling that is associated with cardiac stiffness, mechanical impairment, and vasomotor dysfunction.[11] There is a correlation between cardiac fibrosis and mortality rate in patients with symptomatic HFpEF,[12] so inhibition of cardiac fibrosis may act as a critical measure to improve cardiac function and adverse outcomes.[13] However, due to the complicated heterogeneity in different phenotypes of HFpEF in clinics, the generic pathophysiology of cardiac fibrosis in cardiorenal HFpEF that merely induced by CKD is poorly understood. Characterization of cardiac fibrosis in cardiorenal HFpEF is urgently needed to permit the identification of profibrotic pathways and anti-fibrotic therapies in CKD-induced HFpEF phenotype.[14]

Activation of the renin-angiotensin-aldosterone system (RAAS) is one of the hemodynamic mechanisms that can lead to cardiovascular hypertension, fluid retention, and toxic substance-induced cardiac injury.[15] Angiotensin-converting enzyme inhibitors (ACEIs) and angiotensin II receptor blockers (ARBs) are common RAAS inhibitors for HF therapy. Although trials of ACEIs and ARBs have failed to reduce mortality in patients with HFpEF, and currently no mature pharmacological therapy can improve the prognosis of patients with HFpEF, the use of ARBs is considered to reduce hospitalizations for patients with HFpEF.[5,16,17] Importantly, it has been reported that angiotensin II may be associated with comorbidity-driven myocardial inflammation and increased cardiac fibrosis as well as ECM remodeling in various diseases[18,19]; however, direct evidence of the effects of RAAS modulation on cardiac fibrosis in cardiorenal HFpEF is still lacking.

Thus, the present study aimed to investigate the role of cardiac fibrosis in a rat model of cardiorenal HFpEF and to further explore the potential therapeutic implications of RAAS inhibition with Telmisartan in ameliorating cardiac fibrosis and preserving diastolic function in this model.

Materials and methods

Rat model of cardiorenal HFpEF and animal protocols

All experimental protocols were approved by the Institutional Animal Care and Bioethical Committee of the Medical School of Southeast University (SYXK2015-0036). Male Sprague-Dawley rats weighing 180–220 g were maintained on a 12/12 h light–dark cycle with food and water freely available for one week before the experiments were performed. And 5/6 subtotal nephrectomy (SNX) was performed in rats to induce initial kidney injury by first resecting the whole right kidney and subsequently resecting two-thirds of the left kidney one-week later.[20,21] A group of sham-operated rats was used as control (Sham, $n = 20$). The surgical procedures were conducted under deep anesthesia administered by isoflurane inhalation (Keyuan, Shandong, China). After the surgery, all rats were allowed four weeks to recover and form a stable condition of CKD. Then, the SNX rats were randomly divided into two groups and intragastrically administered vehicle (Veh), which contained 0.5% methylcellulose (SNX + Veh, $n = 20$), or Telmisartan (Tel, 8 mg/kg/d), a standard ARB inhibitor for heart failure (SNX + Tel, $n = 20$) for an additional 12 weeks. Blood and urine collections were performed before the initial surgery of resecting the right kidney as a Baseline value (Baseline, which is one week before 0 w) and on week 4, 8, 12, and 16 after the whole SNX surgery (0 w, which is right after the second surgery of resecting 2/3 of the left kidney) to evaluate renal function. Echocardiography and blood pressure were measured at Baseline and week 16. Cardiac magnetic resonance imaging (MRI) was conducted at week 16. Then, the rats were euthanized, and renal/cardiac pathological examination, real-time PCR, and western blot analysis were performed at week 16 (Figure 1).

Renal function, blood pressure, and brain natriuretic peptide measurement

Blood was acquired from the canthus vein, and 24 h urine samples were collected from all rats in metabolic cages at Baseline before the initial surgery and every four weeks after the whole surgery. Serum creatinine, blood urea nitrogen and 24 h urine protein excretion were separately detected through blood or urine samples to evaluate renal function. According to the protocol, systolic blood pressure and diastolic blood pressure were measured by a noninvasive computerized tail-cuff system (MK-2000; Muromachi Kikai, Tokyo, Japan) in conscious rats at Baseline before the surgery and at week 16 after the SNX surgery. Additionally, blood samples were collected at the same time point for the analysis of brain natriuretic peptide (BNP), and experimental operations were conducted according to kit instructions (Tianjin Anoric Biotechnology, Tianjin, China).

Echocardiography, cardiac magnetic resonance imaging, and function analysis

Trans-thoracic echocardiography was performed with a Vevo 2100 ultrasound system (Visual Sonics, Toronto, Ontario). Both M-mode and two-dimensional short- and long-axis images of the left ventricle were obtained at Baseline before the surgery and at week 16 after the SNX surgery. Parameters of interventricular septal thickness at end-diastole (IVSd), interventricular septal thickness at end-systole (IVSs), left ventricular (LV) posterior wall thickness at end-diastole (LVPWd), LV posterior wall thickness at end-systole (LVPWs), LV end-diastolic volume (LVEDV), LV end-systolic volume (LVESV), EF, and early to late diastolic transmitral flow velocity (E/A) ratio were measured. *In vivo* cardiac MRI was performed in a 7.0 T MR Scanner (Bruker Pharma Scan MRI, Ettlingen, Germany) with respiratory and electrocardiograph double-gated at week 16. Cine images were obtained with a black-blood T1W-Cine

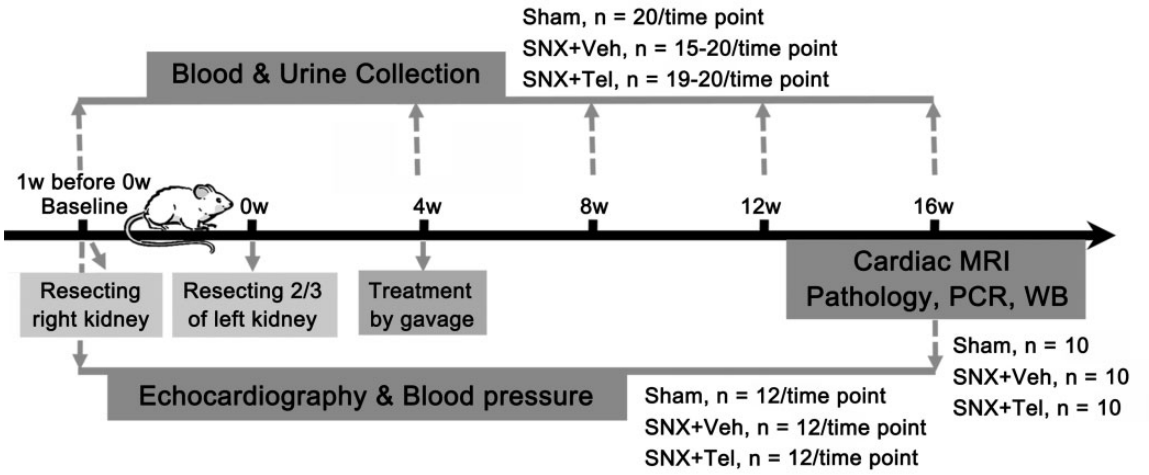

Figure 1. Flowchart of timeline and number of rats used in each group in applied study design. 5/6 subtotal nephrectomy (SNX) was performed in rats to induce initial kidney injury by first resecting the whole right kidney and subsequently resecting two-thirds of the left kidney one week later (0 w, which is right after the whole surgery). A group of sham-operated rats was used as control (Sham). After the surgery, all rats were allowed four weeks to recover and form a stable condition of chronic kidney disease. Then, the SNX rats were randomly divided into two groups and intragastrically administered vehicle (SNX+Veh), or Telmisartan (SNX + Tel) for an additional 12 weeks. Blood and urine collections were performed at Baseline (before the initial surgery, which is one week before 0 w) and on week 4, 8, 12, and 16 after the whole surgery to evaluate renal function. Echocardiography and blood pressure were measured at Baseline before the initial surgery and at week 16 after the whole SNX surgery. Cardiac MRI was conducted at week 16. Then, the rats were euthanized, and renal/cardiac pathological examination, real-time PCR, and western blot analysis were performed at week 16.

FLASH sequence in the axial direction spanning the entire heart in the three groups (Supplementary Movies I–III). A software analysis package (Matlab Analysis, version 6) was used to depict the endocardial and epicardial contours of each slice to produce the myocardial volume–time curve of a cardiac cycle (Supplementary Figure I), and the IVSd, IVSs, LVEDV, LVESV, and EF were derived and measured (Supplementary Table I). A detailed description is provided in the Data Supplement.

Histopathology, real-time PCR, and western blot

After euthanasia, organs of the kidney, heart, liver, lung, and spleen were collected. The tissue sections of the kidney were stained with Masson trichrome for fibrosis and CD68 for macrophages. The tissue sections of the heart were acquired and stained with hematoxylin & eosin (H&E) and Masson trichrome, followed by immunohistochemistry staining with antibodies against α-smooth muscle actin (α-SMA), transforming growth factor (TGF)-β1, connective tissue growth factor (CTGF), and CD68 (Abcam, Cambridge, UK). The fresh cardiac tissues were also acquired for quantitative real-time PCR analysis and western blot analysis of collagen I, collagen III, α-SMA, TGF-β1, and CTGF (Abcam, Cambridge, UK). The expression level of each gene was normalized with GAPDH as an endogenous control, and the signal intensity of the protein levels were normalized to β-actin as an endogenous control. The results were quantified with Image J 1.5 software (NIH, Bethesda, MD, USA). A detailed description is provided in the Data Supplement.

Statistical analysis

The values are reported as the mean ± standard deviation (SD). Statistical comparisons between three groups were performed using a one-way analysis of variance. *Post hoc* analysis with appropriate Bonferroni correction was made. Paired t test was used to compare two groups (the values of Baseline and week 16 in the Sham group). The correlation analysis was performed using Pearson correlation coefficient. Two-sided testing was used. All statistical tests were performed using SPSS software (version 20; SPSS, Chicago, IL), and probability values less than 0.05 were considered significant.

Results

HFpEF phenotype of the subtotal nephrectomy rat model

After the SNX surgery, rats exhibited gradually increased serum creatinine ($P < 0.001$; Figure 2(a)), blood urea nitrogen ($P < 0.001$; Figure 2(b)), and 24 h urine protein excretion ($P < 0.001$; Figure 2(c)) with a trend towards a further increase from week 4 to 16 compared with the Sham group, suggesting chronic renal insufficiency after the SNX surgery. Significantly higher percentage of renal macrophages area ($P < 0.001$; Figure 2(d)) and fibrosis area ($P < 0.001$; Figure 2(e)) were observed in the SNX+Veh group at week 16 compared with the Sham group. In addition, compared with the Sham group at week 16 after the surgery, the SNX+Veh rats at week 16 showed significantly higher systolic blood pressure ($P < 0.001$; Figure 3(a)), diastolic blood pressure ($P < 0.001$; Figure 3(b)), increased BNP levels ($P < 0.001$; Figure 3(c)), and decreased E/A ratio ($P < 0.001$; Figure 3(d) and (e)) as well as preserved ejection fraction ($P =$ NS; Figure 3(f)). No significant differences were observed between the values of Baseline and week 16 in the Sham group ($P =$ NS; Figure 3), demonstrating that within 16 weeks, the changes of the blood pressure, BNP, E/A ratio, and EF did not reach statistical differences

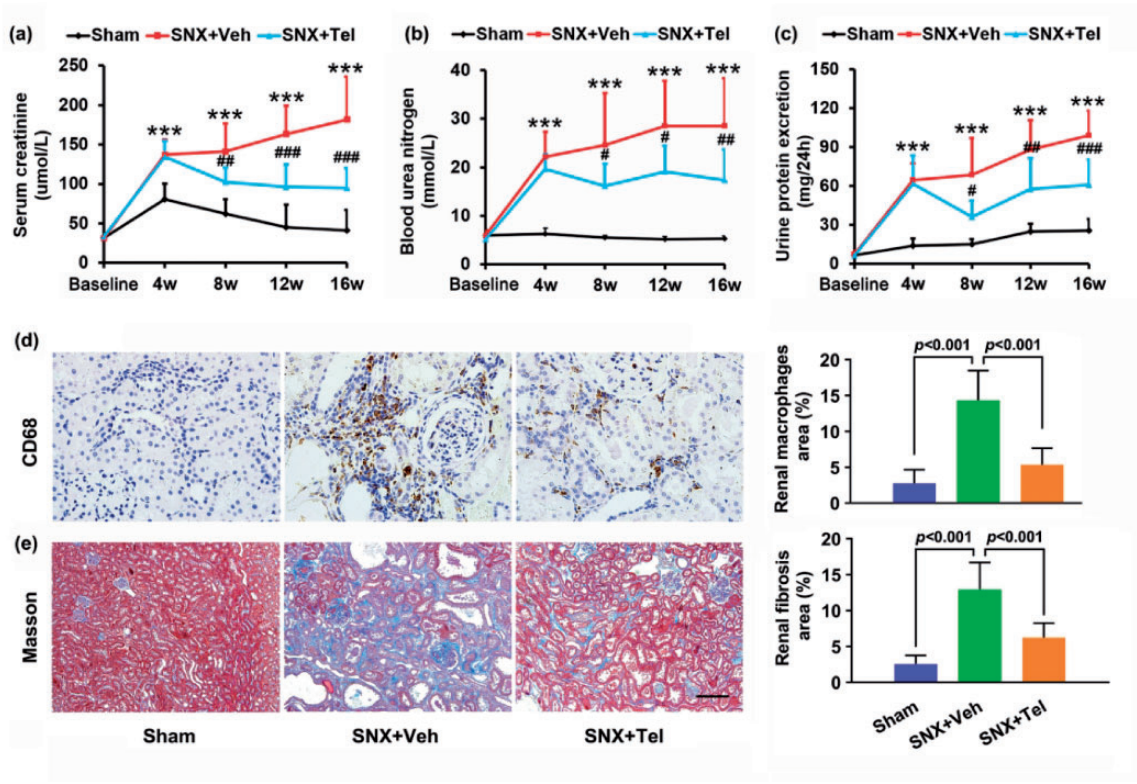

Figure 2. Chronic renal injury in cardiorenal HFpEF and alleviated renal injury after treatment with Telmisartan. The mean ± SD of serum creatinine (a), blood urea nitrogen (b), and 24 h urine protein excretion (c) from Baseline to week 16. (d) Histopathological staining with anti-CD68 and calculated percentages of macrophages in renal sections. (e) Masson staining and calculated percentages of fibrosis in renal sections. Scale bar in (e), 100 μm. *$P < 0.05$, **$P < 0.01$, ***$P < 0.001$ for SNX+Veh vs. Sham; #$P < 0.05$, ##$P < 0.01$, ###$P < 0.001$ for SNX+Veh vs. SNX+Tel. Masson indicates Masson trichrome. (A color version of this figure is available in the online journal.)

in the Sham group. Detailed data of echocardiography and cardiac MRI were provided in Supplementary Table I. The existence of decreased diastolic function and preserved systolic function confirmed the typical signs and symptoms of cardiorenal HFpEF phenotype, in accordance with previous studies as reported by Primessnig *et al.*[22,23]

Alleviated renal injury after treatment with Telmisartan

Compared with the SNX+Veh group, serum creatinine ($P < 0.01$; Figure 2(a)), blood urea nitrogen ($P < 0.05$; Figure 2(b)), and 24 h urine protein excretion ($P < 0.05$; Figure 2(c)) were significantly reduced from week 8 to week 16. Additionally, significantly decreased percentage of renal macrophages area ($P < 0.001$; Figure 2(d)) and fibrosis area ($P < 0.001$; Figure 2(e)) were detected in the SNX + Tel group at week 16. These data indicated that renal failure and injury were improved after long-term treatment with Telmisartan.

Effects of chronic treatment with Telmisartan on cardiorenal HFpEF phenotype and diastolic function

Compared with the vehicle-treated SNX rats, the systolic blood pressure ($P < 0.001$; Figure 3(a)) and diastolic blood pressure ($P = 0.03$; Figure 3(b)) were significantly reduced at week 16 after Telmisartan administration. Also, the BNP values in the SNX + Tel group significantly decreased compared with the SNX+Veh group ($P = 0.0015$; Figure 3 (c)) at week 16. The E/A ratio was significantly increased after chronic Telmisartan treatment ($P = 0.0011$; Figure 3(d) and (e)) at week 16, demonstrating a reversed diastolic function after treatment. Furthermore, no significant differences of the ejection fraction (P = NS; Figure 3(f)) were measured. The features of the HFpEF phenotype following CKD were evidenced by improved diastolic function with no changes of systolic function, and the above results demonstrated that chronic treatment with Telmisartan ameliorated cardiac outcome and diastolic dysfunction in cardiorenal HFpEF.

Left ventricular hypertrophy in cardiorenal HFpEF and reversed hypertrophy after treatment with Telmisartan

Cardiac MRI showed significantly increased IVSd and IVSs as well as decreased LVEDV and LVESV in the SNX+Veh group than the Sham group ($P < 0.001$), which were improved after chronic treatment with Telmisartan ($P < 0.01$; Figure 4(a) to (c)). Echocardiography exhibited significantly increased IVSd, IVSs, LVPWd, and LVPWs as well as decreased LVEDV and LVESV in the SNX+Veh group compared with the Sham group ($P < 0.001$) and the Telmisartan-treated group ($P < 0.05$; Supplementary Figure II(a) to (g)). Pathological examination of the LV H&E staining displayed significantly greater myocyte cross-sectional diameter in the SNX+Veh group than the Sham group

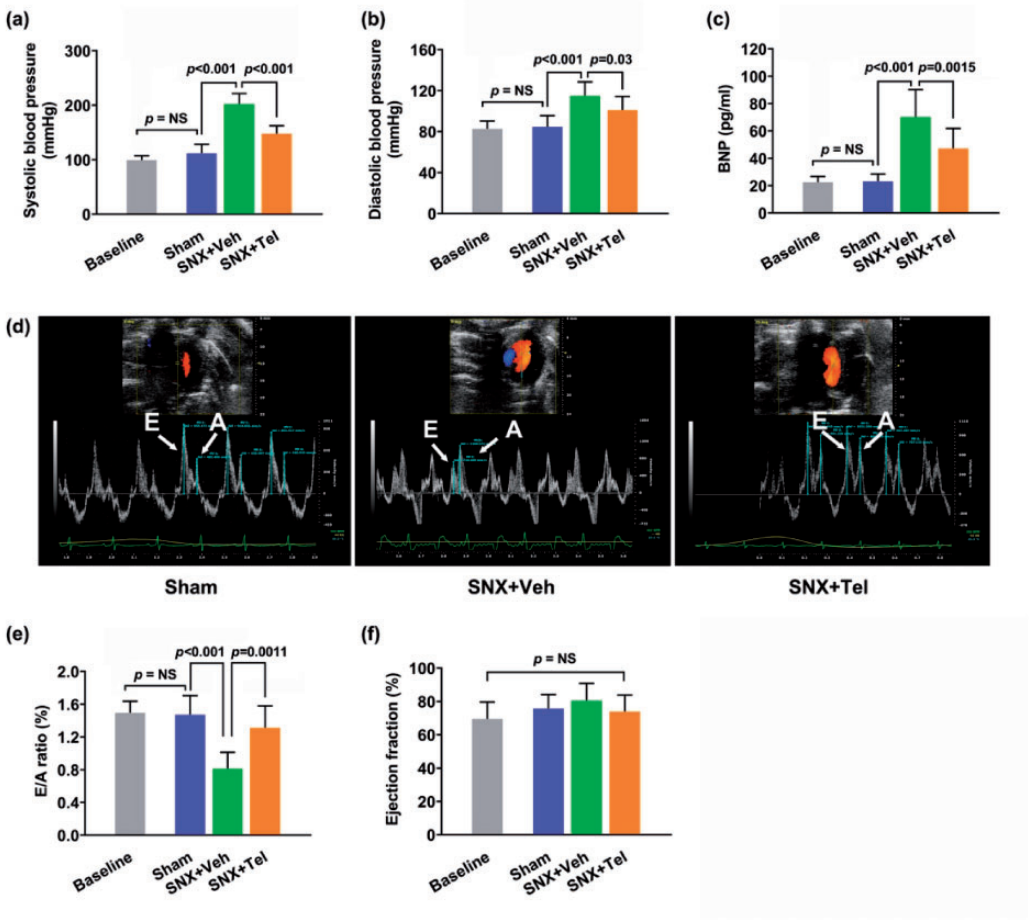

Figure 3. Cardiac function assessment in rats with cardiorenal HFpEF and effects of chronic treatment with Telmisartan on cardiorenal HFpEF phenotype. The mean ± SD of systolic blood pressure (a), diastolic blood pressure (b), and BNP (c) at Baseline and at week 16 after the surgery. The E/A ratio in echocardiography at week 16 (d) and the quantified mean ± SD of E/A ratio (e), and ejection fraction (f) at Baseline and at week 16 after the surgery. BNP indicates brain natriuretic peptide; E/A: early to late diastolic transmitral flow velocity. (A color version of this figure is available in the online journal.)

($P < 0.001$) and Telmisartan-treated group ($P = 0.002$; Figure 4(d)). Chronic treatment with Telmisartan also showed significantly reduced LV mass than the SNX+Veh group ($P = 0.034$; Figure 4(e)). All these results demonstrated increased LV hypertrophy in the SNX+Veh group than the Sham group, and long-term treatment with Telmisartan could reversed LV hypertrophy in cardiorenal HFpEF rats (Figure 4; Supplementary Figure II and Supplementary Table I).

Characterization of cardiac fibrosis in cardiorenal HFpEF and reduced cardiac fibrosis, collagen I/III and profibrotic cytokines after treatment with Telmisartan

Significantly increased cardiac fibrosis was observed in the SNX+Veh group compared with the Sham group at week 16 by Masson trichrome staining ($P < 0.001$), whereas chronic treatment with Telmisartan significantly reduced cardiac fibrosis compared with the SNX+Veh rats ($P = 0.0017$; Figure 5(a) and (b)). Quantitative real-time PCR (Figure 5(c)) and western blot (Figure 5(d)) showed significantly increased protein expression of collagen I and collagen III in the SNX+Veh group compared with the Sham group and Telmisartan-treated group ($P < 0.05$). Within the same tissues of LV, positive staining for profibrotic cytokines of α-SMA, TGF-β1, and CTGF were markedly increased in the SNX+Veh group compared with the Sham group and SNX + Tel group (Figure 6(a)). Quantitative analysis of real-time PCR (Figure 6(b)) and western blot (Figure 6(c)) showed significantly increased protein expression of α-SMA, TGF-β1, and CTGF in the SNX+Veh group compared with the Sham rats ($P < 0.05$), whereas chronic treatment with Telmisartan significantly decreased these protein expressions ($P < 0.05$). The above data indicated that cardiac fibrosis and its markers (collagen I, collagen III, and profibrotic cytokines) were prominent in the pathology of cardiorenal HFpEF and implicated decreased cardiac fibrosis as a possible contributing factor to the beneficial effects of long-term Telmisartan treatment.

Reduced cardiac inflammation after treatment with Telmisartan and the correlation between cardiac inflammation and fibrosis in cardiorenal HFpEF

The number of inflammatory cells in H&E staining (Figure 7(a)) and macrophages in CD68 immunohistochemical staining (Figure 7(b)) were higher in the SNX+Veh group than the Sham group and Telmisartan-treated group at week 16. Quantitative analysis revealed significantly increased percentage of macrophage-positive area

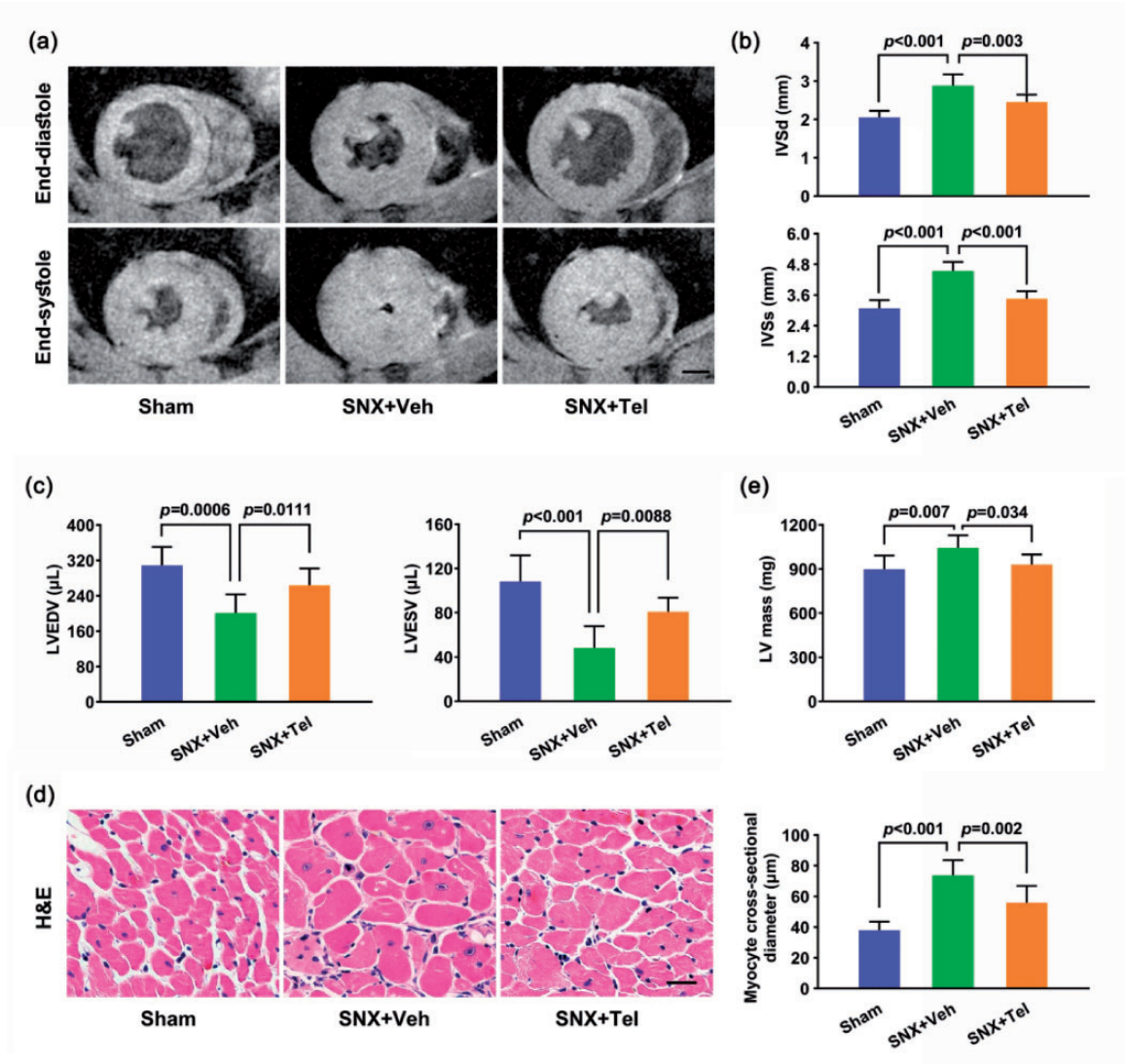

Figure 4. Left ventricular hypertrophy measurement by cardiac MRI and histology. (a) Cardiac Cine MRI of the same slice of the heart at end-diastole (top row) and end-systole (bottom row) of the three groups at week 16 and (b) the mean ± SD of IVSd and IVSs as well as (c) the mean ± SD of LVEDV and LVESV at week 16 after the surgery. (d) Cardiac H&E staining of myocytes in cross-section at week 16 and the calculated mean ± SD of myocyte cross-sectional diameter. (e) The mean ± SD of LV mass at week 16. Scale bar in (a), 2.5 mm. Scale bar in (d), 50 μm. MRI indicates magnetic resonance imaging; IVSd: interventricular septal thickness at end-diastole; IVSs: interventricular septal thickness at end-systole; LVEDV: left ventricular end-diastolic volume; LVESV: left ventricular end-systolic volume; H&E: hematoxylin & eosin; LV: left ventricular. (A color version of this figure is available in the online journal.)

in the myocardium ($P < 0.001$), which was markedly reduced after chronic Telmisartan treatment ($P = 0.009$; Figure 7(c)). Intriguingly, the fibrotic area (Masson) was in close proximity with the macrophage-positive area (CD68) in consecutive slices (Figure 7(d)), and there was a linear correlation between the percentage of macrophage-positive area and the fibrosis area ($R^2 = 0.68$; $P < 0.001$; Figure 7(e)), suggesting that inflammatory macrophages were associated with accumulated fibrosis in cardiorenal HFpEF. Furthermore, we also did immunohistochemical staining of CD68 positive macrophages and α-SMA positive myofibroblasts in consecutive slices (Figure 8), and observed that although they existed in the same clusters of cells of the myocardium, they did not overlap, indicating that perhaps the accumulation of macrophages in the myocardium contributed to the recruitment of myofibroblasts. In addition, CD68 immunohistochemical staining and Masson trichrome staining of the kidney, heart, lung, liver, and spleen showed increased macrophages and fibrosis in all these organs in the SNX+Veh group than the Sham group at week 16, which were more prominent in the kidney and heart (Supplementary Figure II), indicating that there may be a systemic proinflammatory state that potentially led to tissue fibrosis in the rat model of cardiorenal HFpEF, especially the cardiac inflammatory–fibrosis alterations and ECM remodeling.

Discussion

In the present study, we demonstrated that cardiorenal HFpEF is associated with increased cardiac fibrosis, and RAAS modulation with Telmisartan could ameliorate cardiac fibrosis and improve diastolic dysfunction in cardiorenal HFpEF.

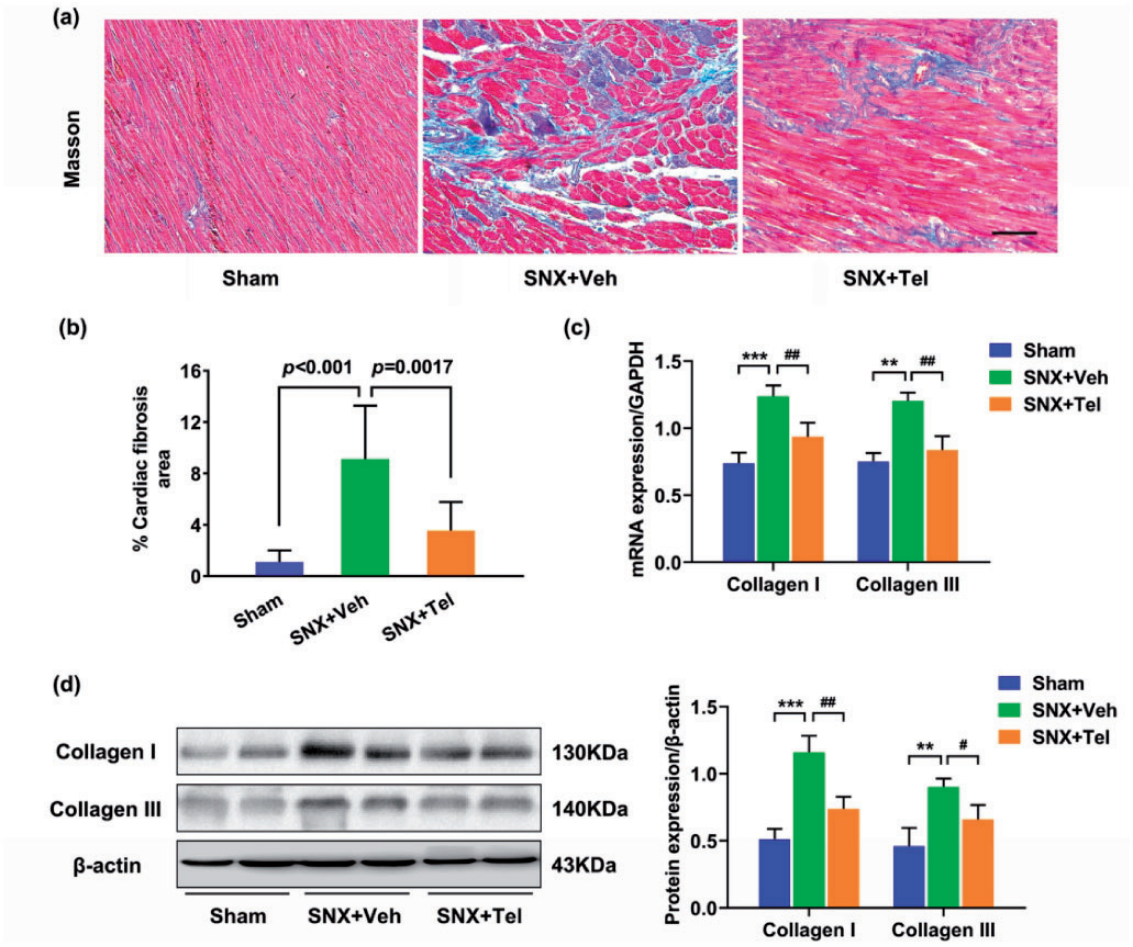

Figure 5. Characterization of cardiac fibrosis in cardiorenal HFpEF and reduced cardiac fibrosis and collagen deposition after treatment with Telmisartan. (a) Masson staining and (b) the calculated mean ± SD of percentage of cardiac fibrosis at week 16. (c) Real-time PCR and (d) western blotting of collagen I and collagen III in heart tissues at week 16 and the calculated mean ± SD of protein/β-actin ratios of collagen I and collagen III. Scale bar in (a), 100 μm. $^{*}P < 0.05$, $^{**}P < 0.01$, $^{***}P < 0.001$ for SNX+Veh vs. Sham; $\#P < 0.05$, $\#\#P < 0.01$, $\#\#\#P < 0.001$ for SNX+Veh vs. SNX+Tel. (A color version of this figure is available in the online journal.)

Epidemiological data have shown that the five-year survival rate of HFpEF is only 35%, whereas efficient therapies to improve the outcome of HFpEF remain challenging.[4,5,24] At present, HFpEF is still an ill-defined clinical entity and the categorization in association with its own pathophysiological phenotype is poorly understood.[25–27] As a systemic disorder, CKD has been proven to be associated independently with cardiac dysfunction, and CKD-associated mortality was even higher in HFpEF than in HFrEF.[10,28,29] This phenotype of HFpEF is now called cardiorenal HFpEF, which owns the features of clinical HFpEF syndrome. Nevertheless, studies on cardiorenal HFpEF caused by chronic renal dysfunction is far from sufficient, making it a key defect in choosing the right treatment for the right patient. As CKD is a main driver of HFpEF, we hereby performed a rat model of 5/6 SNX with a cardiorenal HFpEF phenotype. Impaired diastolic function (E/A ratio), elevated BNP, and cardiac hypertrophy were investigated, while the systolic function (EF) of heart was maintained in this rat model, which were in consistent with previous studies and the diagnostic criteria for HFpEF.[16,22,23,30]

Cardiac fibrosis may play an essential role in the development of HFpEF.[31,32] Currently, data are emerging to support the hypothesis that biomarkers of cardiac fibrosis can be predictive of clinical hospitalization and mortality and may provide incremental prognostic value over BNP in patients with HF,[33] and diagnostic emphasis of HFpEF should be redirected to enhanced inflammation and interstitial fibrosis so as to halt and perhaps reverse pathology.[8,34] Nonetheless, the explicit pathogenesis, particularly the contribution of cardiac fibrosis in cardiorenal-associated HFpEF, is yet to be conclusively proven. To evaluate the role of cardiac fibrosis in cardiorenal HFpEF, we investigated cardiac fibrosis in CKD-induced HFpEF and observed that the percentage of fibrosis area, markers of fibrosis (collagen I, collagen III), and profibrotic cytokines (α-SMA, TGF-β1 and CTGF) were all increased in cardiac tissues in the vehicle-treated HFpEF group than the Sham-operated rats. Exacerbated LV hypertrophy and diastolic dysfunction were also observed in cardiorenal HFpEF rats than the Sham animals by using echocardiography and cardiac MRI. Considering that excess collagen deposition and ECM remodeling may lead to LV hypertrophy and

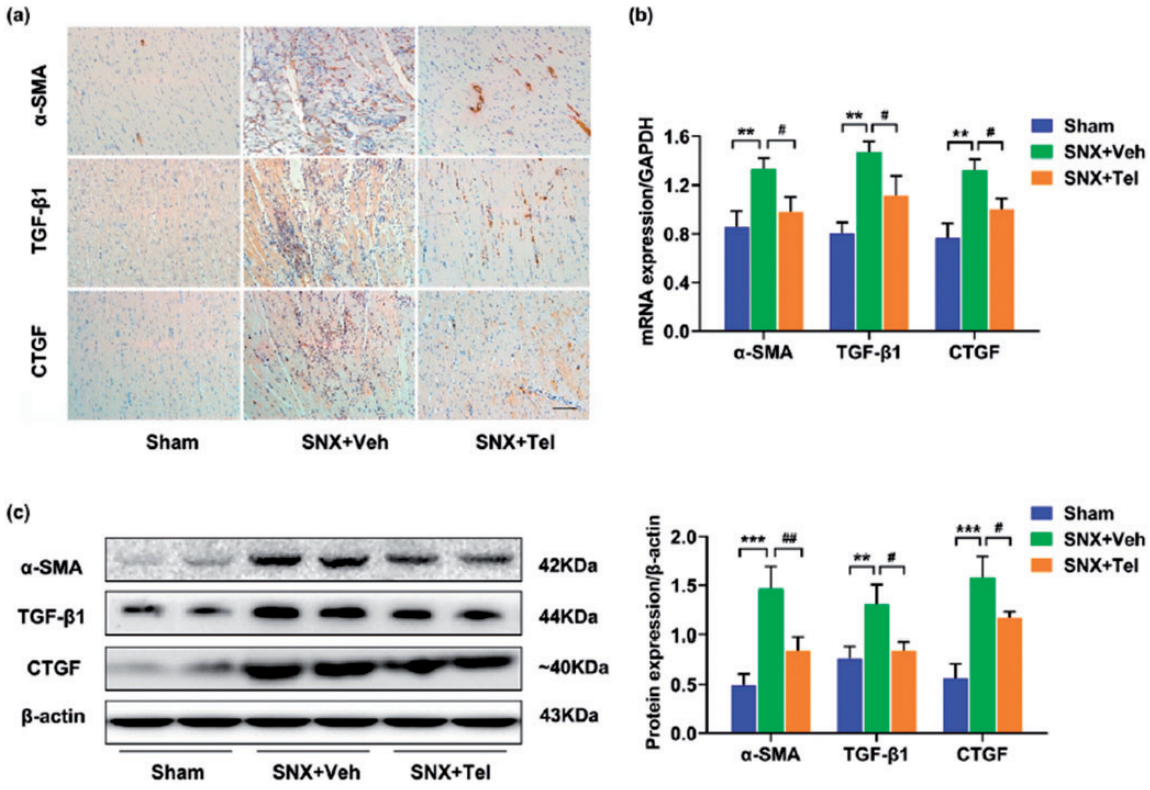

Figure 6. Characterization of cardiac profibrotic cytokines expression in cardiorenal HFpEF. (a) Immunohistochemical staining of α-SMA, TGF-β1, and CTGF at week 16. (b) Real-time PCR and (c) western blot of α-SMA, TGF-β1, and CTGF in heart tissues and the calculated mean ± SD of protein/β-actin ratios. Scale bar in (a), 100 μm. *$P < 0.05$, **$P < 0.01$, ***$P < 0.001$ for SNX+Veh vs. Sham; #$P < 0.05$, ##$P < 0.01$, ###$P < 0.001$ for SNX+Veh vs. SNX+Tel. (A color version of this figure is available in the online journal.)

stiffening, cardiac fibrosis might promote decreased myocardial compliance and diastolic dysfunction in cardiorenal HFpEF. It is recognized that fibrosis is a common consequence of inflammatory response in organ injury[31]; thus, we still investigated cardiac inflammation and observed massive inflammatory cells and macrophages infiltrating the myocardium in the vehicle-treated HFpEF group, and the percentage of macrophage-positive area was correlated with the percentage of fibrosis area in the heart. The CD68 staining of various organs (kidney, heart, lung, liver, and spleen) revealed a wide distribution but different amounts of macrophages in these organs, suggesting that there is a systemic inflammatory state in cardiorenal HFpEF that potentially contribute to the development of cardiac fibrosis.[35,36] Recent studies revealed that myocardial inflammation can trigger expression of TGF-β and stimulates myofibroblasts to deposit collagen, acting as a key driver of cardiac fibrosis and LV remodeling in HFpEF.[37,38] These insights may support a reset of therapeutic targets by modulating the inflammatory–fibrosis response in cardiorenal HFpEF.[4]

ACEIs and ARBs are common RAAS inhibitors in treating HF in clinics, predominantly systolic hypertension.[17] Meta-analysis revealed that RAAS inhibitors can improve the prognosis of patients with HFrEF, but cannot improve outcomes of patients with HFpEF, perhaps due to the complexity of multiple complications in clinical practice such as worsened renal function.[39] Although RAAS inhibitors can usually cause a decline of renal function in HFpEF patients, this decline is often small and will not lead to treatment interruption.[16] Since the therapeutic benefits of RAAS inhibitors may be largely maintained in patients with cardiorenal HFpEF, the underling pharmacological mechanisms of RAAS inhibitors in associated with the elusive pathogenesis of cardiorenal HFpEF require in-depth research. Here, the therapeutic implications of Telmisartan were investigated in cardiorenal HFpEF that merely induced by CKD. Long-term treatment with Telmisartan ameliorated cardiac fibrosis, collagen I, collagen III, profibrotic cytokines, and inflammation as well as reversed cardiac hypertrophy in HFpEF rats, demonstrating that chronic Telmisartan administration may play a key role in the regulation of fibrotic remodeling and structural alterations in cardiorenal HFpEF. Moreover, alleviated diastolic dysfunction was shown in this model, suggesting an effect of Telmisartan in reversing cardiac functional alterations, which might possibly by blocking the activation of profibrotic cytokines and myofibroblasts as well as preventing the deposition of collagen in cardiorenal HFpEF. Altogether, the current study employed Telmisartan to verify the therapeutic effects of RAAS modulation in cardiorenal HFpEF and demonstrated that Telmisartan may exert an intriguing therapeutic implication through the inhibition of inflammatory–fibrosis process, which might be a promising therapeutic strategy for cardiorenal HFpEF in clinical practice.

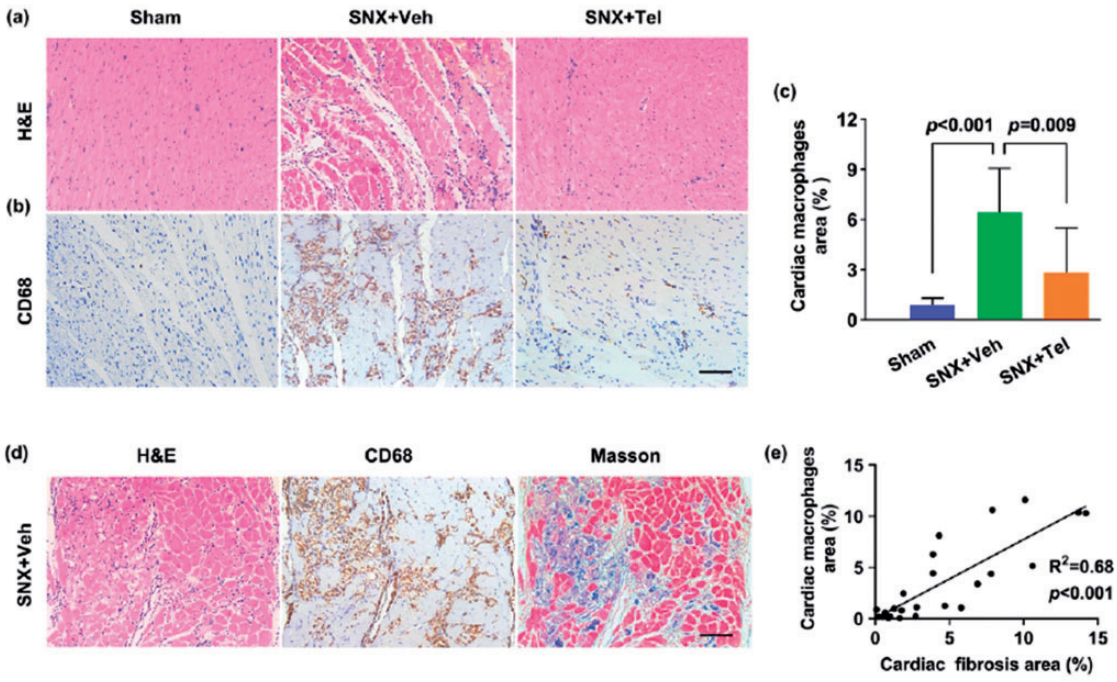

Figure 7. Reduced cardiac inflammation after treatment with Telmisartan and correlation analysis of cardiac inflammation and fibrosis. (a) Cardiac H&E staining and (b) CD68 immunohistochemical staining at week 16 and (c) the calculated mean ± SD of percentage of cardiac macrophages at week 16. (d) Cardiac inflammatory cells (H&E, left), macrophages (CD68, middle), and fibrosis (Masson, right) in adjacent cardiac slices and (e) the quantitative correlation analysis between percentage of macrophages area and percentage of fibrosis area ($R^2 = 0.68$; $P < 0.001$). Scale bar in (b) and (d), 100 μm. H&E indicates hematoxylin & eosin; Masson: Masson trichrome. (A color version of this figure is available in the online journal.)

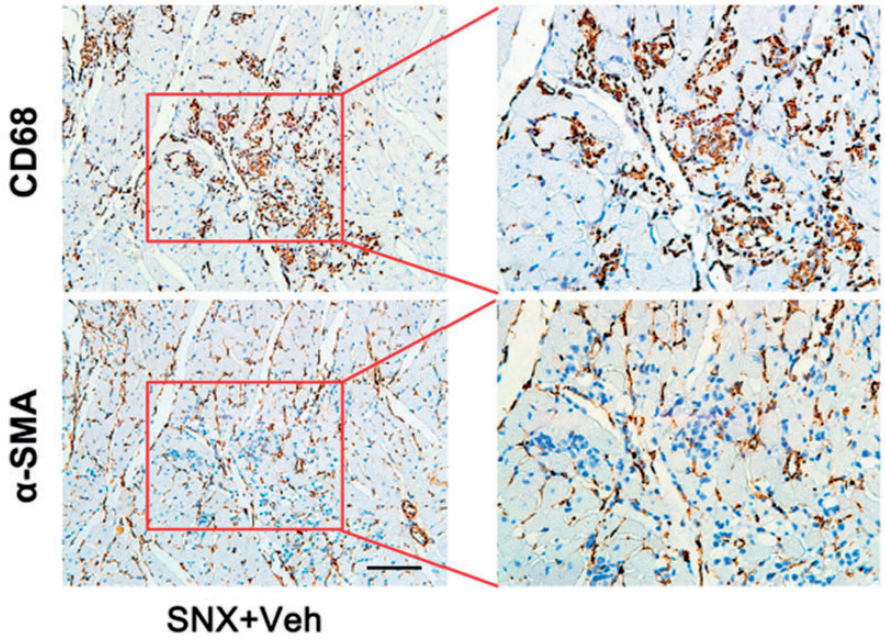

Figure 8. Immunohistological staining of macrophages and myofibroblasts in adjacent cardiac slices. Cardiac tissues of the SNX+Veh rats at week 16 were stained sequentially with anti-CD68 and α-SMA in adjacent slices. Although CD68-positive macrophages and α-SMA-positive myofibroblasts coexisted in the same clusters, they did not overlap. Scale bar, 100 μm. (A color version of this figure is available in the online journal.)

Our study had several limitations. Firstly, we did not determine a combined effect of hypertension and excessive fibrosis in deteriorating cardiac structural and functional alterations in cardiorenal HFpEF, and the initial step of CKD-induced inflammatory–fibrosis process remains unknown in the current study. It is possible that other initial activation mechanisms might have contributed to heart dysfunction in cardiorenal HFpEF. In addition, we did not use variables other than E/A ratio for identifying diastolic dysfunction. Several other recommended variables

such as early filling (E) and early diastolic mitral annular velocity (e′) ratio (E/e′ ratio) and IVRT can also be used to evaluate diastolic dysfunction, but different variables have different disadvantages, and the E/A ratio is a feasible and reproducible clinical variable to provide diagnostic information of diastolic dysfunction. Finally, we cannot deny that the modulation of RAAS may induce other hemodynamic or histopathological alterations in addition to the regulation of fibrosis and inflammation.

In conclusion, the present study demonstrated that cardiac fibrosis may play a central role in the pathology of cardiorenal HFpEF by using a rat model of CKD-induced HFpEF phenotype. In addition, the modulation of RAAS with Telmisartan was capable of alleviating LV remodeling and diastolic dysfunction possibly via the inhibition of cardiac inflammatory–fibrosis process in the development of cardiorenal HFpEF.

AUTHORS' CONTRIBUTIONS

DC, SHJ, TTX, SJZ, YC conceptualized the problem; DC, SHJ developed an experimental method; DC, SDM, ZZ conducted the experiments; DC, TTX, YC did a literature research; DC wrote the manuscript; DC, TTX, CQL collected resources; DC, YCW reviewed and edited; SHJ, YCW supervised.

DECLARATION OF CONFLICTING INTERESTS

The author(s) declared no potential conflicts of interest with respect to the research, authorship, and/or publication of this article.

FUNDING

The author(s) disclosed receipt of the following financial support for the research, authorship, and/or publication of this article: This work was supported by the National Natural Science Foundation of China (NSFC, No. 81801759), Natural Science Foundation of Jiangsu Province (BK20180375, BK20190355), Science Foundation for Creative Research Groups of the Ministry of Science and Technology of China (No. 6290002012), National Natural Science Foundation of China (NSFC, Nos. 81830053, 81601465, 81901809).

ORCID iD

Shenghong Ju https://orcid.org/0000-0001-5041-7865

SUPPLEMENTAL MATERIAL

Supplemental material for this article is available online.

REFERENCES

1. Clark KA, Velazquez EJ. Heart failure with preserved ejection fraction: time for a reset. *JAMA* 2020;**324**:1506–8
2. Hahn VS, Knutsdottir H, Luo X, Bedi K, Margulies KB, Haldar SM, Stolina M, Yin J, Khakoo AY, Vaishnav J, Bader JS, Kass DA, Sharma K. Myocardial gene expression signatures in human heart failure with preserved ejection fraction. *Circulation* 2021;**143**:120–34
3. Pfeffer MA, Shah AM, Borlaug BA. Heart failure with preserved ejection fraction in perspective. *Circ Res* 2019;**124**:1598–617
4. Shah SJ, Borlaug BA, Kitzman DW, McCulloch AD, Blaxall BC, Agarwal R, Chirinos JA, Collins S, Deo RC, Gladwin MT, Granzier H, Hummel SL, Kass DA, Redfield MM, Sam F, Wang TJ, Desvigne-Nickens P, Adhikari BB. Research priorities for heart failure with preserved ejection fraction: national heart, lung, and blood institute working group summary. *Circulation* 2020;**141**:1001–26
5. Yancy CW, Jessup M, Bozkurt B, Butler J, Casey DE Jr, Colvin MM, Drazner MH, Filippatos GS, Fonarow GC, Givertz MM, Hollenberg SM, Lindenfeld J, Masoudi FA, McBride PE, Peterson PN, Stevenson LW, Westlake C. 2017 ACC/AHA/HFSA focused update of the 2013 ACCF/AHA guideline for the management of heart failure: a report of the American College of Cardiology/American Heart Association task force on clinical practice guidelines and the heart failure society of America. *Circulation* 2017;**136**:e137–61
6. Schiattarella GG, Altamirano F, Tong D, French KM, Villalobos E, Kim SY, Luo X, Jiang N, May HI, Wang ZV, Hill TM, Mammen PP, Huang J, Lee DI, Hahn VS, Sharma K, Kass DA, Lavandero S, Gillette TG, Hill JA. Nitrosative stress drives heart failure with preserved ejection fraction. *Nature* 2019;**568**:351–6
7. Shah SJ, Kitzman DW, Borlaug BA, van Heerebeek L, Zile MR, Kass DA, Paulus WJ. Phenotype-specific treatment of heart failure with preserved ejection fraction: a multiorgan roadmap. *Circulation* 2016;**134**:73–90
8. Lam CS, Voors AA, de Boer RA, Solomon SD, van Veldhuisen DJ. Heart failure with preserved ejection fraction: from mechanisms to therapies. *Eur Heart J* 2018;**39**:2780–92
9. Zannad F, Rossignol P. Cardiorenal syndrome revisited. *Circulation* 2018;**138**:929–44
10. Ahmed A, Rich MW, Sanders PW, Perry GJ, Bakris GL, Zile MR, Love TE, Aban IB, Shlipak MG. Chronic kidney disease associated mortality in diastolic versus systolic heart failure: a propensity matched study. *Am J Cardiol* 2007;**99**:393–8
11. Sweeney M, Corden B, Cook SA. Targeting cardiac fibrosis in heart failure with preserved ejection fraction: mirage or miracle? *EMBO Mol Med* 2020;**12**:e10865
12. Kanagala P, Cheng ASH, Singh A, Khan JN, Gulsin GS, Patel P, Gupta P, Arnold JR, Squire IB, Ng LL, McCann GP. Relationship between focal and diffuse fibrosis assessed by CMR and clinical outcomes in heart failure with preserved ejection fraction. *JACC Cardiovasc Imaging* 2019;**12**:2291–301
13. Cunningham JW, Claggett BL, O'Meara E, Prescott MF, Pfeffer MA, Shah SJ, Redfield MM, Zannad F, Chiang LM, Rizkala AR, Shi VC, Lefkowitz MP, Rouleau J, McMurray JJV, Solomon SD, Zile MR. Effect of sacubitril/valsartan on biomarkers of extracellular matrix regulation in patients with HFpEF. *J Am Coll Cardiol* 2020;**76**:503–14
14. Luscher TF. Heart failure with preserved ejection fraction: towards an understanding of an enigma. *Eur Heart J* 2019;**40**:3277–80
15. Zaritsky JJ, Kalantar-Zadeh K. The crossroad of RAAS modulation, inflammation, and oxidative stress in dialysis patients: light at the end of the tunnel? *J Am Soc Nephrol* 2012;**23**:189–91
16. Ponikowski P, Voors AA, Anker SD, Bueno H, Cleland JG, Coats AJ, Falk V, Gonzalez-Juanatey JR, Harjola VP, Jankowska EA, Jessup M, Linde C, Nihoyannopoulos P, Parissis JT, Pieske B, Riley JP, Rosano GMC, Ruilope LM, Ruschitzka F, Rutten FH, van der Meer P, Group ESCSD. 2016 ESC guidelines for the diagnosis and treatment of acute and chronic heart failure: the task force for the diagnosis and treatment of acute and chronic heart failure of the European Society of Cardiology (ESC) developed with the special contribution of the heart failure association (HFA) of the ESC. *Eur Heart J* 2016;**37**:2129–200
17. Shah RV, Desai AS, Givertz MM. The effect of renin-angiotensin system inhibitors on mortality and heart failure hospitalization in patients with heart failure and preserved ejection fraction: a systematic review and meta-analysis. *J Card Fail* 2010;**16**:260–7
18. Rosner MH, Ronco C, Okusa MD. The role of inflammation in the cardio-renal syndrome: a focus on cytokines and inflammatory mediators. *Semin Nephrol* 2012;**32**:70–8
19. Kudo H, Kai H, Kajimoto H, Koga M, Takayama N, Mori T, Ikeda A, Yasuoka S, Anegawa T, Mifune H, Kato S, Hirooka Y, Imaizumi T. Exaggerated blood pressure variability superimposed on hypertension

aggravates cardiac remodeling in rats via angiotensin II system-mediated chronic inflammation. *Hypertension* 2009;**54**:832–8
20. Zhu X, Callahan MF, Gruber KA, Szumowski M, Marks DL. Melanocortin-4 receptor antagonist TCMCB07 ameliorates cancer- and chronic kidney disease-associated cachexia. *J Clin Invest* 2020;**130**:4921–34
21. Chang D, Wang YC, Zhang SJ, Bai YY, Liu DF, Zang FC, Wang G, Wang B, Ju S. Visualizing myocardial inflammation in a rat model of type 4 cardiorenal syndrome by dual-modality molecular imaging. *Biomaterials* 2015;**68**:67–76
22. Primessnig U, Bracic T, Levijoki J, Otsomaa L, Pollesello P, Falcke M, Pieske B, Heinzel FR. Long-term effects of Na(+)/Ca(2+) exchanger inhibition with ORM-11035 improves cardiac function and remodelling without lowering blood pressure in a model of heart failure with preserved ejection fraction. *Eur J Heart Fail* 2019;**21**:1543–52
23. Rieger AC, Bagno LL, Salerno A, Florea V, Rodriguez J, Rosado M, Turner D, Dulce RA, Takeuchi LM, Kanashiro-Takeuchi RM, Buchwald P, Wanschel A, Balkan W, Schulman IH, Schally AV, Hare JM. Growth hormone-releasing hormone agonists ameliorate chronic kidney disease-induced heart failure with preserved ejection fraction. *Proc Natl Acad Sci USA* 2021;**118**:e2019835118
24. Byrne NJ, Matsumura N, Maayah ZH, Ferdaoussi M, Takahara S, Darwesh AM, Levasseur JL, Jahng JW, Vos D, Parajuli N, El-Kadi AO, Braam B, Young ME, Verma S, Light PE, Sweeney G, Seubert JM, Dyck JR. Empagliflozin blunts worsening cardiac dysfunction associated with reduced NLRP3 (nucleotide-binding domain-like receptor protein 3) inflammasome activation in heart failure. *Circ Heart Fail* 2020;**13**:e006277
25. Obokata M, Reddy YN, Borlaug BA. Diastolic dysfunction and heart failure with preserved ejection fraction: understanding mechanisms by using noninvasive methods. *JACC Cardiovasc Imaging* 2020;**13**:245–57
26. Kitzman DW, Upadhya B, Vasu S. What the dead can teach the living: systemic nature of heart failure with preserved ejection fraction. *Circulation* 2015;**131**:522–4
27. Borlaug BA. The pathophysiology of heart failure with preserved ejection fraction. *Nat Rev Cardiol* 2014;**11**:507–15
28. Fang JC. Heart failure with preserved ejection fraction: a kidney disorder? *Circulation* 2016;**134**:435–7
29. Damman K, Tang WH, Felker GM, Lassus J, Zannad F, Krum H, McMurray JJ. Current evidence on treatment of patients with chronic systolic heart failure and renal insufficiency: practical considerations from published data. *J Am Coll Cardiol* 2014;**63**:853–71
30. Primessnig U, Schonleitner P, Holl A, Pfeiffer S, Bracic T, Rau T, Kapl M, Stojakovic T, Glasnov T, Leineweber K, Wakula P, Antoons G, Pieske B, Heinzel FR. Novel pathomechanisms of cardiomyocyte dysfunction in a model of heart failure with preserved ejection fraction. *Eur J Heart Fail* 2016;**18**:987–97
31. Mohammed SF, Hussain S, Mirzoyev SA, Edwards WD, Maleszewski JJ, Redfield MM. Coronary microvascular rarefaction and myocardial fibrosis in heart failure with preserved ejection fraction. *Circulation* 2015;**131**:550–9
32. Zile MR, Baicu CF, Ikonomidis JS, Stroud RE, Nietert PJ, Bradshaw AD, Slater R, Palmer BM, Van Buren P, Meyer M, Redfield MM, Bull DA, Granzier HL, LeWinter MM. Myocardial stiffness in patients with heart failure and a preserved ejection fraction: contributions of collagen and titin. *Circulation* 2015;**131**:1247–59
33. Lopez B, Ravassa S, Gonzalez A, Zubillaga E, Bonavila C, Berges M, Echegaray K, Beaumont J, Moreno MU, San Jose G, Larman M, Querejeta R, Diez J. Myocardial collagen cross-linking is associated with heart failure hospitalization in patients with hypertensive heart failure. *J Am Coll Cardiol* 2016;**67**:251–60
34. Bayes-Genis A, de Antonio M, Vila J, Penafiel J, Galan A, Barallat J, Zamora E, Urrutia A, Lupon J. Head-to-head comparison of 2 myocardial fibrosis biomarkers for long-term heart failure risk stratification: ST2 versus galectin-3. *J Am Coll Cardiol* 2014;**63**:158–66
35. Paulus WJ. Unfolding discoveries in heart failure. *N Engl J Med* 2020;**382**:679–82
36. Redfield MM. Heart failure with preserved ejection fraction. *N Engl J Med* 2016;**375**:1868–77
37. Dobaczewski M, Bujak M, Li N, Gonzalez-Quesada C, Mendoza LH, Wang XF, Frangogiannis NG. Smad3 signaling critically regulates fibroblast phenotype and function in healing myocardial infarction. *Circ Res* 2010;**107**:418–28
38. Loredo-Mendoza ML, Ramirez-Sanchez I, Bustamante-Pozo MM, Ayala M, Navarrete V, Garate-Carrillo A, Ito BR, Ceballos G, Omens J, Villarreal F. The role of inflammation in driving left ventricular remodeling in a pre-HFpEF model. *Exp Biol Med (Maywood)* 2020;**245**:748–57
39. Beldhuis IE, Streng KW, Ter Maaten JM, Voors AA, van der Meer P, Rossignol P, McMurray JJ, Damman K. Renin-angiotensin system inhibition, worsening renal function, and outcome in heart failure patients with reduced and preserved ejection fraction: a meta-analysis of published study data. *Circ Heart Fail* 2017;**10**:e003588

(Received April 7, 2021, Accepted July 2, 2021)